Title
How well do CMIP5 climate simulations replicate historical trends and patterns of meteorological droughts?

Journal
Water Resources Research, 51(4)

ISSN
0043-1397

Authors
Nasrollahi, N
Aghakouchak, A
Cheng, L
et al.

Publication Date
2015-04-01

DOI
10.1002/2014WR016318

AGU PUBLICATIONS

Water Resources Research

RESEARCH ARTICLE

10.1002/2014WR016318

How well do CMIP5 climate simulations replicate historical trends and patterns of meteorological droughts?

Nasrin Nasrollahi[1], Amir AghaKouchak[1], Linyin Cheng[1], Lisa Damberg[1], Thomas J. Phillips[2], Chiyuan Miao[3], Kuolin Hsu[1], and Soroosh Sorooshian[1]

[1]Center for Hydrometeorology and Remote Sensing, University of California, Irvine, California, USA, [2]Lawrence Livermore National Laboratory, Livermore, California, USA, [3]College of Global Change and Earth System Science, Beijing Normal University, Beijing, China

Key Points:
- CMIP5 model simulations overestimate precipitation falling at lower rates
- Most ensemble members overestimate the areas under extreme drought
- Most CMIP5 models do not agree with observed regional drying and wetting trends

Supporting Information:
- Supporting Information S1

Correspondence to:
N. Nasrollahi,
nasrin.n@uci.edu

Citation:
Nasrollahi, N., A. AghaKouchak, L. Cheng, L. Damberg, T. J. Phillips, C. Miao, K. Hsu, and S. Sorooshian (2015), How well do CMIP5 climate simulations replicate historical trends and patterns of meteorological droughts?, *Water Resour. Res.*, *51*, 2847–2864, doi:10.1002/2014WR016318.

Received 21 AUG 2014
Accepted 24 MAR 2015
Accepted article online 28 MAR 2015
Published online 26 APR 2015

Abstract Assessing the uncertainties and understanding the deficiencies of climate models are fundamental to developing adaptation strategies. The objective of this study is to understand how well Coupled Model Intercomparison-Phase 5 (CMIP5) climate model simulations replicate ground-based observations of continental drought areas and their trends. The CMIP5 multimodel ensemble encompasses the Climatic Research Unit (CRU) ground-based observations of area under drought at all time steps. However, most model members overestimate the areas under extreme drought, particularly in the Southern Hemisphere (SH). Furthermore, the results show that the time series of observations and CMIP5 simulations of areas under drought exhibit more variability in the SH than in the Northern Hemisphere (NH). The trend analysis of areas under drought reveals that the observational data exhibit a significant positive trend at the significance level of 0.05 over all land areas. The observed trend is reproduced by about three-fourths of the CMIP5 models when considering total land areas in drought. While models are generally consistent with observations at a global (or hemispheric) scale, most models do not agree with observed regional drying and wetting trends. Over many regions, at most 40% of the CMIP5 models are in agreement with the trends of CRU observations. The drying/wetting trends calculated using the 3 months Standardized Precipitation Index (SPI) values show better agreement with the corresponding CRU values than with the observed annual mean precipitation rates. Pixel-scale evaluation of CMIP5 models indicates that no single model demonstrates an overall superior performance relative to the other models.

1. Introduction

Drought is a complex condition that develops more slowly than other extreme weather and climate phenomena, such as floods, hurricanes, and tornadoes. Droughts are considered among the most costly natural disasters due to their impacts on crop yield, infrastructure, industry, and tourism [*Wilhite*, 2000]. In recent years, major droughts have affected the United States, East Africa, Russia, and Brazil with significant adverse impacts across different sectors [*Hoerling et al*., 2013, 2014; *AghaKouchak et al*., 2014; *Funk*, 2011]. For investigation of meteorological drought, it is necessary to examine the changes in both precipitation and occurrence frequency. Numerous studies show increases in the frequency and severity of droughts under prospective climate change scenarios [*Wehner*, 2012; *Sheffield and Wood*, 2008; *Dai*, 2012]. *Alexander and Arblaster* [2009] highlighted the importance of validating climate simulations with respect to historical observations when attempting to project future dry spells. The ability of a climate model to estimate present climate and reproducing historical trends leads to higher confidence in projecting future climate [*Reifen and Toumi*, 2009; *Wuebbles et al*., 2014].

Recently, the Climate Modeling Intercomparison Project has provided the Phase 5 (CMIP5) multimodel simulations of both historical (1850–2005) and prospective future (21st century) climates corresponding to different greenhouse-gas (GHG) emissions scenarios [*Taylor et al*., 2012]. The CMIP5 models represent the most recent collective attempt to predict the spatiotemporal evolution of the coupled ocean-land-atmosphere components of the global climate system on a centennial time scale. Several studies have evaluated the CMIP5 precipitation simulations at regional and global scales [e.g., *Sheffield et al*., 2013; *Joetzjer et al*., 2012; *Yin et al*., 2013; *Hao et al*., 2013; *Schubert and Lim*, 2013; *Sillmann et al*., 2013; *Pascale et al*., 2014; *Feng et al*., 2013; *Balan Sarojini et al.,* 2012; *Kharin et al.,* 2013]. *Mehran et al*. [2014] investigated the accuracy and bias

of CMIP5 historical simulations of total precipitation, and of its upper quartile, compared to the Global Precipitation Climatology Project (GPCP). They showed that despite good agreement in overall patterns of precipitation between the multimodel ensemble mean and the observations, the upper quartile of simulated precipitation amount does not compare well in most parts of the globe. They concluded that, while in most regions the total precipitation simulated by CMIP5 models are in fair agreement with GPCP observations, some desert and high-latitude regions exhibit large discrepancies.

A recent study showed that the pattern of dry-day frequency of the historical CMIP5 simulations ensemble mean is in good agreement with the GPCP data [*Polade et al*., 2014]. The same study confirmed better results over land in comparison to oceans, as expected due to more accurate observations over land. On the regional scale, *Yin et al*. [2013] highlighted an underestimation of precipitation over Amazonia by most CMIP5 models. In addition, the CMIP5 historical data in arid and semiarid areas were found to underestimate annual precipitation amounts, with large intermodel variations over arid and semiarid regions [*ZHao et al*., 2014]. *Liu et al*. [2014] investigated the bias in CMIP5 data over eight regions with distinct seasonal climates, and confirmed differences in the regional and seasonal performance of the CMIP5 model simulations. *Wuebbles et al*. [2013] showed that most CMIP5 model data underestimate 4–6 month drought in central and western North America, while over eastern North America the model results are in better agreement with drought observations of the past 30 years. *Ault et al*. [2012] noted that the decadal to multidecadal variability of precipitation was generally too low in CMIP5 simulations, especially over arid to semiarid regions and the Amazon. They emphasized the importance of understanding model weaknesses in simulating processes that generate precipitation fluctuations, in order to improve future models.

The CMIP5 simulations have been used to analyze droughts in the past and future climate [e.g., *Cai et al*., 2014; *Fu et al*., 2013; *Orlowsky and Seneviratne*, 2013; *Prudhomme et al*., 2014]. In recent years, discrepancies between climate model-based and ground-based precipitation trends were reported [see *Sheffield et al*., 2012; *Damberg and AghaKouchak*, 2014; *Trenberth et al*., 2014]. The objective of the present study is to investigate how well CMIP5 simulations of historical climate replicate observed trends and patterns of drought at a global scale, as represented by the Climatic Research Unit (CRU) observational data set.

The focus of this study is on meteorological droughts, defined in terms of precipitation deficits, as measured by the Standardized Precipitation Index (SPI) [*McKee et al*., 1993; *Hayes et al*., 1999], whose advantages as a drought indicator are well understood [e.g., *Hayes et al*., 2011]. Using SPI data derived from CMIP5 climate simulations and CRU observations, the present study quantitatively addresses the following research questions: relative to the CRU observations, how well do CMIP5 climate simulations replicate (a) historical drought areas; (b) significant trends in the spatial extent of these droughts; (c) associated wetting and drying regions; and (d) precipitation distribution function. This paper is organized as follows: section 2 summarizes the features of different data sets used in this study, while section 3 describes the analysis methodology. Section 4 presents detailed results, with conclusions provided in section 5.

2. Data Sets

Historical monthly precipitation simulations by 41 CMIP5 models for the period 1901–2005 are processed for this drought analysis. These represent multimodel simulations of historical climate conditions that are contributions to the World Climate Research Programme's CMIP5 data set collections [*Meehl and Bony*, 2011; *Taylor et al*., 2012]. The CMIP5 simulations of historical climate analyzed in this study are listed in Table 1. It should be noted that model names including the suffix "_esm" are coupled earth systems models (ESMs) that have prognostic carbon-cycle capabilities. For these historical simulations of climate, however, such capabilities were "switched off," and the ESMs were forced by prescribed historical time series of atmospheric greenhouse-gas *emissions*, as distinct from other CMIP5 models that were forced by the historical time series of greenhouse-gas *concentrations* [*Taylor et al*., 2012].

Monthly precipitation observations from the Climatic Research Unit (CRU) [*New et al*., 2000; *Mitchell and Jones*, 2005] are used as reference data. Both CRU observations and CMIP5 multimodel simulations are remapped onto a common $2^\circ \times 2^\circ$ grid for comparison, with the focus on global land areas between 90°N and 75°S. We acknowledge that CRU ground based is subject to uncertainties and biases that could affect the evaluation, particularly over remote regions in Africa, South America, and Asia, where ground-based

Table 1. H Values From the Mann-Kendall Statistical Significance Test for CMIP5 Model Simulations of Areas in Drought (6 Month SPI ≤ -1) Over Global Land Areas ("Land"), and of Those Only in the Northern Hemisphere (NH) and in the Southern Hemisphere (SH)[a]

	p = 0.05 (95% Confidence Level)				p = 0.05 (95% Confidence Level)		
	Land	NH	SH		Land	NH	SH
CRU	1	1	1	GISS-E2-H	1	1	1
BCC-CSM1-1-esm	1	1	0	GISS-E2-R	1	1	1
BCC-CSM1-1	1	1	1	HadGEM2-CC	1	0	1
CanESM2-esm	0	0	1	HadGEM2-ES-esm	0	1	1
CanESM2	0	0	1	HadGEM2-ES	1	0	1
CCSM4	1	1	1	INMCM4-esm	1	1	1
CESM1-BGC-esm	1	1	0	IPSL-CM5A-LR-esm	1	1	0
CESM1-BGC	1	1	1	IPSL-CM5A-LR	1	1	0
CESM1-CAM5	0	0	1	IPSL-CM5A-MR	1	1	0
CESM1-FASTCHEM	1	1	0	IPSL-CM5B-LR	1	1	1
CESM1-WACCM	1	1	0	MIROC5	1	1	1
CNRM-CM5	1	1	1	MIROC-ESM-CHEM	1	1	0
CSIRO-ACCESS1-0	1	0	1	MIROC-ESM-esm	1	1	0
CSIRO-ACCESS1–3	0	1	0	MIROC-ESM	1	0	1
CSIRO-Mk3–6-0	1	1	0	MPI-ESM-LR-esm	1	1	1
FGOALS-g2	1	1	1	MPI-ESM-LR	1	1	1
FGOALS-s2	1	1	1	MPI-ESM-P	0	1	1
GFDL-CM3	1	1	1	MRI-CGCM3	1	1	1
GFDL-ESM2G-esm	0	0	0	MRI-ESM1-esm	1	1	1
GFDL-ESM2M-esm	0	1	1	NorESM1-M	1	1	0
GFDL-ESM2M	1	1	1	NorESM1-ME	1	1	1

[a]The detection of a significant drying trend is indicated by "1," and no significant drying trend by a "0."

measurements are limited [*New et al*., 1999, 2000; *Tanarhte et al*., 2012; *Hao et al*., 2013]. For this reason, most of the results are provided for post-1950 for which more reliable data are available [*New et al*., 1999].

It should be noted that while there are several other global drought data records based on ground-based data or combined satellite and ground-based observations [e.g., *Hao et al*., 2014; *AghaKouchak and Nakhjiri*, 2012], these only provide three to four decades of observational data. Such records are insufficient for a reliable evaluation of the CMIP5 simulations, which cannot be expected to reproduce the details of the time series of historical monthly/annual climate observations. This is mainly because these details strongly depend on sea surface temperatures that are predicted by the coupled models, rather than being prescribed from historical oceanic observations [*Peterson et al*., 2012; *Kenyon and Hegerl*, 2010]. Since the CMIP5 models can only reproduce the long-term observational statistics, this study focuses on analyzing the consistency of trends in CMIP5 simulations and ground-based observations at a centennial time scale.

3. Methodology

In this study, we focus on meteorological droughts, defined as deficit in precipitation [*Wilhite*, 2000]. The most commonly used indicator of meteorological droughts is the Standardized Precipitation Index (SPI) recommended by the World Meteorological Organization for drought assessment [*McKee et al*., 1993; *Hayes et al*., 2011]. To avoid any assumption regarding the underlying distribution function of precipitation, a nonparametric method outlined in *Farahmand and AghaKouchak* [2015] is used for deriving SPI [see also *Hao et al*., 2014]. Then, SPI data, derived from both historical CMIP5 simulations and CRU observations, are used to identify areas under drought for different drought severity thresholds. SPI shows precipitation for any given period relative to its climatological average in the standard normal scale. An area under drought is defined as where the 6 month SPI ≤ -1, which is a commonly used threshold for locating instances of moderate drought severity [*McKee et al*., 1993]. To identify extreme droughts, a common threshold of SPI ≤ -2, which corresponds to exceptional drought severity in the U.S. Drought Monitor, is used [*Svoboda et al*., 2002].

In order to investigate the trends in the areas under drought, the nonparametric test developed by Mann-Kendall [*Mann*, 1945; *Kendall*, 1976] is employed. Having a vector of precipitation data as $x_1, \ldots, x_n$, the test evaluates the rank of each value with all the other observation ranks. The test, which should be performed on statistically independent samples, relies solely on the ranks of the samples ($x_1, \ldots, x_n$), and does not

consider their actual values. While annual precipitation data sets can be considered statistically independent observations, this is not the case on a subannual scale (e.g., 3 and 6 month SPI). To address this issue at subannual scales, nonoverlapping data are sampled from the entire data record. For example, when analyzing 6 month SPI, two 6 month observations of January to June and July to December estimates are used for trend analysis. This approach has been used for drought analysis in previous studies [e.g., *Golian et al*., 2014; *Damberg and AghaKouchak*, 2014]. In this test, the so-called S-statistic is defined as:

$$S = \sum_{i=1}^{n-1} \sum_{j=i+1}^{n} \mathrm{sgn}(x_j - x_i) \tag{1}$$

where

$$\mathrm{sgn}(x_j - x_i) \begin{cases} +1, & (x_j - x_i) > 0 \\ 0, & (x_j - x_i) = 0 \\ -1, & (x_j - x_i) < 0 \end{cases} \tag{2}$$

where *sgn* corresponds to the sign function. In equation (2), for a positive difference between any two values (e.g., x_j and x_i), the S-statistic (equation (1)) is increased by +1. For a negative difference, on the other hand, the S-statistic is decreased by −1. In the Mann-Kendall test, a large positive S-statistic implies an increasing trend, whereas a large negative value indicates a decreasing trend. The statistical significance of the observed trend can be tested using the so-called *Z* test approach [*Yue et al*., 2002; *Fatichi*, 2009]:

$$Z = \begin{cases} \dfrac{S-1}{\sqrt{\dfrac{n(n-1)(2n+5) - \sum_{j=1}^{q} t_j(t_j-1)(2t_j+5)}{18}}}, & \text{if } S > 0 \\ 0, & \text{if } S = 0 \\ \dfrac{S+1}{\sqrt{\dfrac{n(n-1)(2n+5) - \sum_{j=1}^{q} t_j(t_j-1)(2t_j+5)}{18}}}, & \text{if } S < 0 \end{cases} \tag{3}$$

where *n* sample size;

q number of ties in the data set;

t_j number of data in the *j*th tie group.

The statistical significance of the observed trends has been assessed at the 95% confidence level, which corresponds to a 5% significance level ($\alpha = 0.05$) that is commonly used in the hydrological sciences. The null-hypothesis (H_0) that there is no significant trend in the data cannot be rejected if the *p* value of the test exceeds the significance level (here), while a *p* value less than the significance level indicates the presence of a statistically significant trend in the data (see H values listed in Table 1).

In addition to the trends, the consistency of the precipitation distribution functions of the CMIP5 simulations and CRU observations are evaluated using the Kullback-Leibler (KL) divergence test [*Kullback and Leibler*, 1951]. This concept is central to the information theory and often used as a measure of discrepancy between two density distributions [*Dragalin et al*., 2003]. The KL test is based on the principle of minimum cross entropy, also known as relative entropy, and can potentially be used for change detection in hydrology and climatology [*AghaKouchak*, 2014]. The KL test measures the distance of one distribution to another (here CMIP5 simulations relative to the CRU observations) based on the entropy concept. The minimum cross entropy indicates whether the two distributions are different at a 0.05 significance level (i.e., 95% confidence level). The KL test has been used in speech and image recognition, machine learning, and neuroscience [*Pérez-Cruz*, 2008]. However, its application to hydroclimatology remains rare.

Assuming F and G as two distributions with densities f and g, representing CMIP5 model simulations and ground-based observations, the Kullback-Leibler divergence (D_{KL}) can be described as:

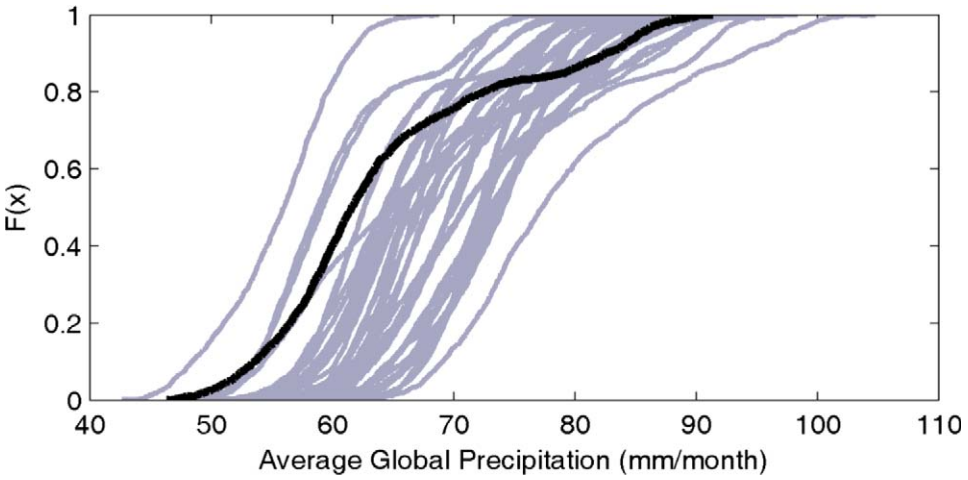

Figure 1. Empirical CDF of the average global monthly precipitation rate (in mm/month) for CRU observations (in black) and for individual CMIP5 simulations (in gray).

$$D_{KL}(f,\ g) = E_f \log \frac{f(X)}{g(X)} \tag{4}$$

where X is the variable of interest (here precipitation); E_f indicates the expectation over the distribution f. For discrete probability distributions $f = \{f_1, \ldots, f_n\}$ and $g = \{g_1, \ldots, g_n\}$, the D_{KL} is defined as:

$$D_{KL}(f,\ g) = \sum_{i}^{n} f_i \log \frac{f_i}{g_i} \tag{5}$$

For values of D_{KL}, one can obtain the likelihood ratio test to detect significant divergence (here test the null-hypothesis that the two distributions are statistically similar at 95% significant level). In this study, D_{KL} is the likelihood ratio between CMIP5 precipitation simulations and the reference CRU observations.

4. Results and Discussion

The empirical Cumulative Distribution Functions (CDFs) of the average global monthly precipitation for the CMIP5 simulations and the CRU observations are provided in Figure 1. The figure clearly shows that for any given quantile (e.g., 0.1, 0.2) light rain values (e.g., precipitation less than 70 mm/month) in most CMIP5 models are larger than in the observations. This could be because of the model "drizzle phenomenon" that has been extensively studied by *Liu et al*. [2014] for different regions and seasons. On the other hand, for high quantiles (e.g., 0.8, 0.9), intense precipitation values in most of the CMIP5 models are smaller than in the CRU observations (Figure 1).

The areas under drought (6 month SPI ≤ -1) for (a) all land areas, (b) land areas in the Northern Hemisphere (NH), and (c) land areas in the Southern Hemisphere (SH) are shown in Figure 2. The gray lines indicate the 41 CMIP5 climate model simulations and the black line indicates the CRU observations. For reference, the ensemble mean of all CMIP5 models is indicated by a solid blue line. As shown, the envelope of climate model simulations encompasses the CRU observations at most time points. A visual comparison indicates the larger variability in SPI values based on CRU observations in the SH than in the NH, as confirmed by the respective hemispheric-average standard deviations (STDs) of CRU-based areas under drought (5.90% versus 3.99%). Overall, the CMIP5 climate model simulations reproduce this hemispheric difference in variability reasonably well. The spatial differences (at pixel scale) of areas under drought among CMIP5 simulations are discussed later in this section.

In model simulations, the range of area under drought in the NH varies between 3% and 36%, while in the SH area under drought exceeds 50% in some of the model simulations (Figure 2). This indicates that model simulations exhibit higher variability in SH (STDs vary between 4.27 and 8.32) compared to the NH (STDs vary between 3.24 and 5.07). The maximum observed area under drought in CRU observations are 28% and

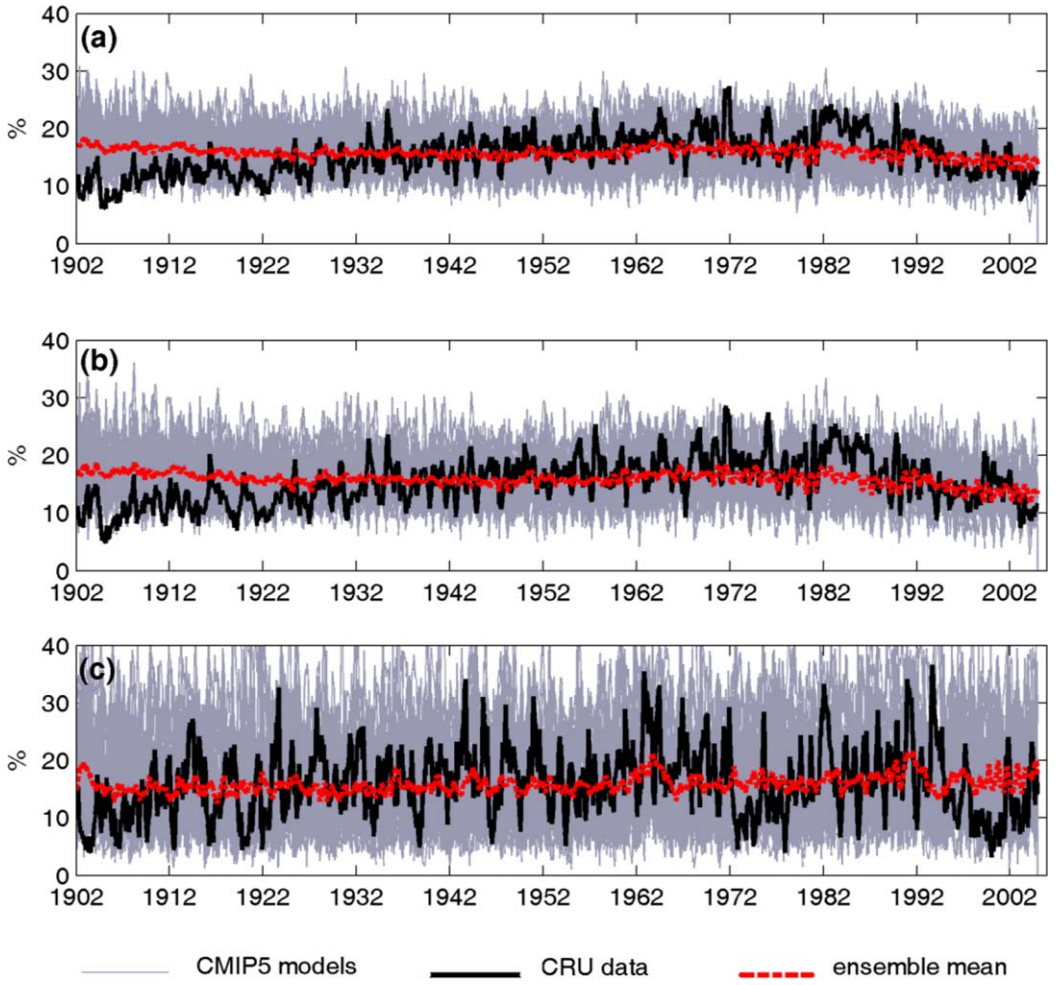

Figure 2. Percentage of land area (%) under drought (6 month SPI ≤ -1) from 1902 to 2005 for: (a) total land areas, (b) land areas in the Northern Hemisphere, and (c) land areas in the Southern Hemisphere. Values derived from CRU precipitation observations are shown in black, the values from the ensemble of 41 CMIP5 simulations are shown in gray, and the red line denotes the ensemble mean of these simulations.

37% for NH and SH, respectively. This result implies that model simulations exhibit substantially higher variability compared to observations, especially in the SH (compare SH CRU STD of 5.90 with STDs of model simulations ranging 4.27–8.32).

Figure 3 presents areas under severe drought (SPI ≤ -2) for (a) all land areas, (b) land areas in the NH, and (c) land areas in the SH. As in Figure 2, the temporal variability of areas under extreme drought in simulations substantially exceeds those derived from the CRU observations. One can see that the area observed under extreme drought has not exceeded 5% in the NH, while the range of variability in model simulations is 3 times higher (see also the NH STD of CRU observation 0.92 as opposed to STDs of model simulations ranging 0.95–1.29). In Figure 3, CMIP5 multimodel simulations encompass the observations at most (but not all) time steps during the period 1901–2005, but they substantially overestimate the area under extreme drought (SPI ≤ -2), especially in the SH where the temporal variability is generally larger (e.g., compare SH CRU STD of 1.58 with STDs of model simulations ranging 1.31–2.63). In CMIP5 simulations, the area under extreme droughts in the NH is never greater than 15%, while in the SH it exceeds 20% at several time steps. This behavior of model simulations is consistent with the CRU-based observations of the NH and SH area under drought (i.e., range of observed area under extreme drought is nearly twice as high in the SH compared to the NH). To ensure consistency of the results, the statistics of areas under moderate and extreme droughts based on the 3 month SPI data are provided in supporting information (see Figures S1 and S2). As shown, the results are consistent with those based on the 6 month SPI.

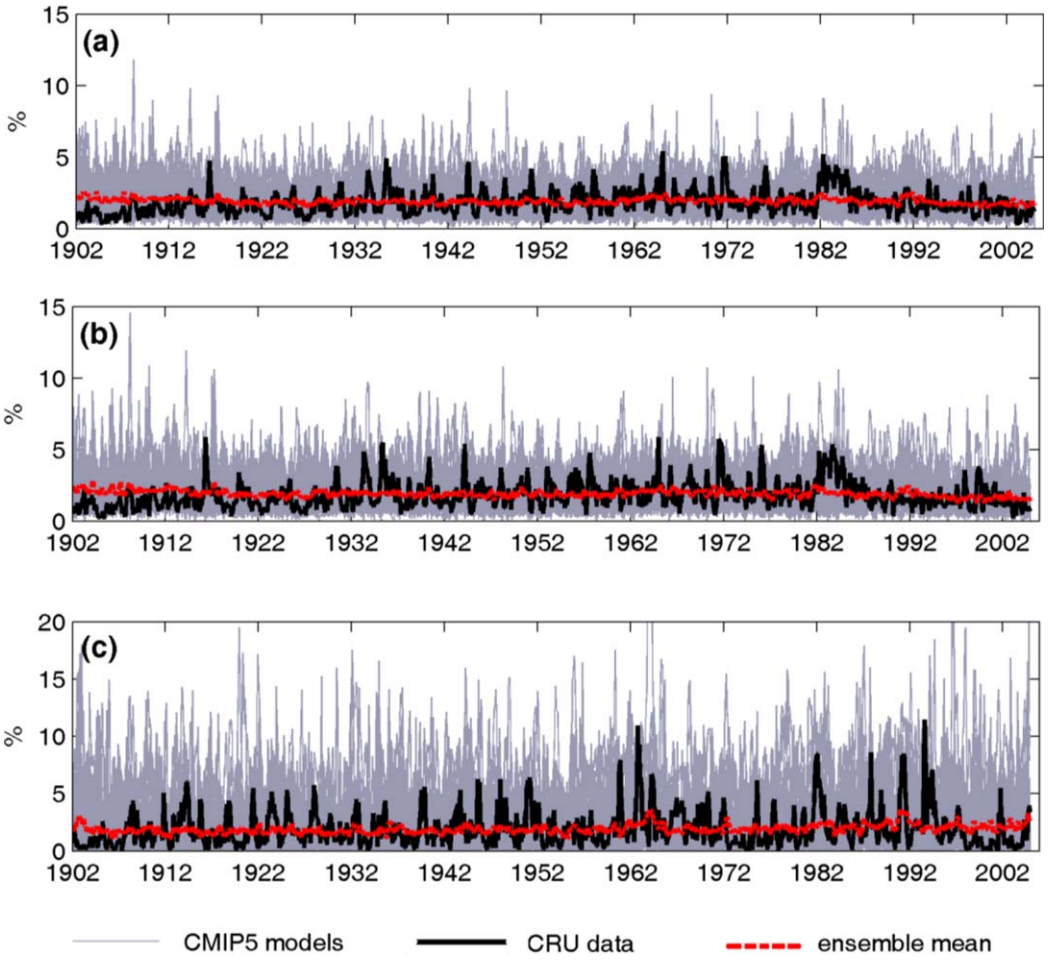

Figure 3. Percentage of land area (%) under severe drought conditions (6 month SPI ≤ -2) from 1902 to 2005 for: (a) total land areas, (b) land areas in the NH, and (c) land areas in the SH. Black lines denote the values derived from the CRU observations, gray shading the envelope of the 41 CMIP5 simulations considered, and the red line their ensemble mean.

This study finds that the CRU observational time series of area under drought shows a significant ($\alpha = 0.05$) positive trend for all land areas, both NH and SH (see Table 1, where an H value of 0 indicates that the null-hypothesis of no trend cannot be rejected, whereas an H value of 1 corresponds to a statistically significant trend at a 95% confidence level). This observation is reproduced by 32 (78%) of the 41 CMIP5 simulations. When considering the NH and the SH separately, 32 (78%) and 27 (66%) of the CMIP5 climate simulations confirm the observed significant trends (see Table 1, columns 3 and 4, respectively). Thus, overall the results indicate that a large majority of the CMIP5 simulations agree in the sign of both global and hemispheric precipitation trends derived from the CRU observations. It should also be noted that the "_esm" models in which the historical time series of greenhouse gas *emissions* are prescribed do not exhibit systematically different patterns from the rest of the model simulations wherein greenhouse gas *concentrations* instead are specified. That is, the ESM simulations of historical climate are not systematically better or worse than those of other CMIP5 models in detecting drought trends.

Regional trend analysis is an important issue in understanding historical changes in precipitation extremes. Previous studies highlighted regional differences in precipitation frequency and changes in the CMIP5 model simulations [*Liu et al*., 2014]. In order to investigate the spatial pattern of droughts, this study investigates the wetting and drying trends of annual mean precipitation. For a more reliable trend analysis, only the period 1950–2005 is considered, since there are more ground-based observations after 1950 [*Becker et al*., 2013; *Vittal et al*., 2013; *New et al*., 2000]. Figure 4a displays the statistically significant drying (red) and wetting (blue) trends in the CRU observations. Most of the regions with significant positive (wetting) trend occur in the United States, South America, northern Europe, Western Australia, and central Asia. On the

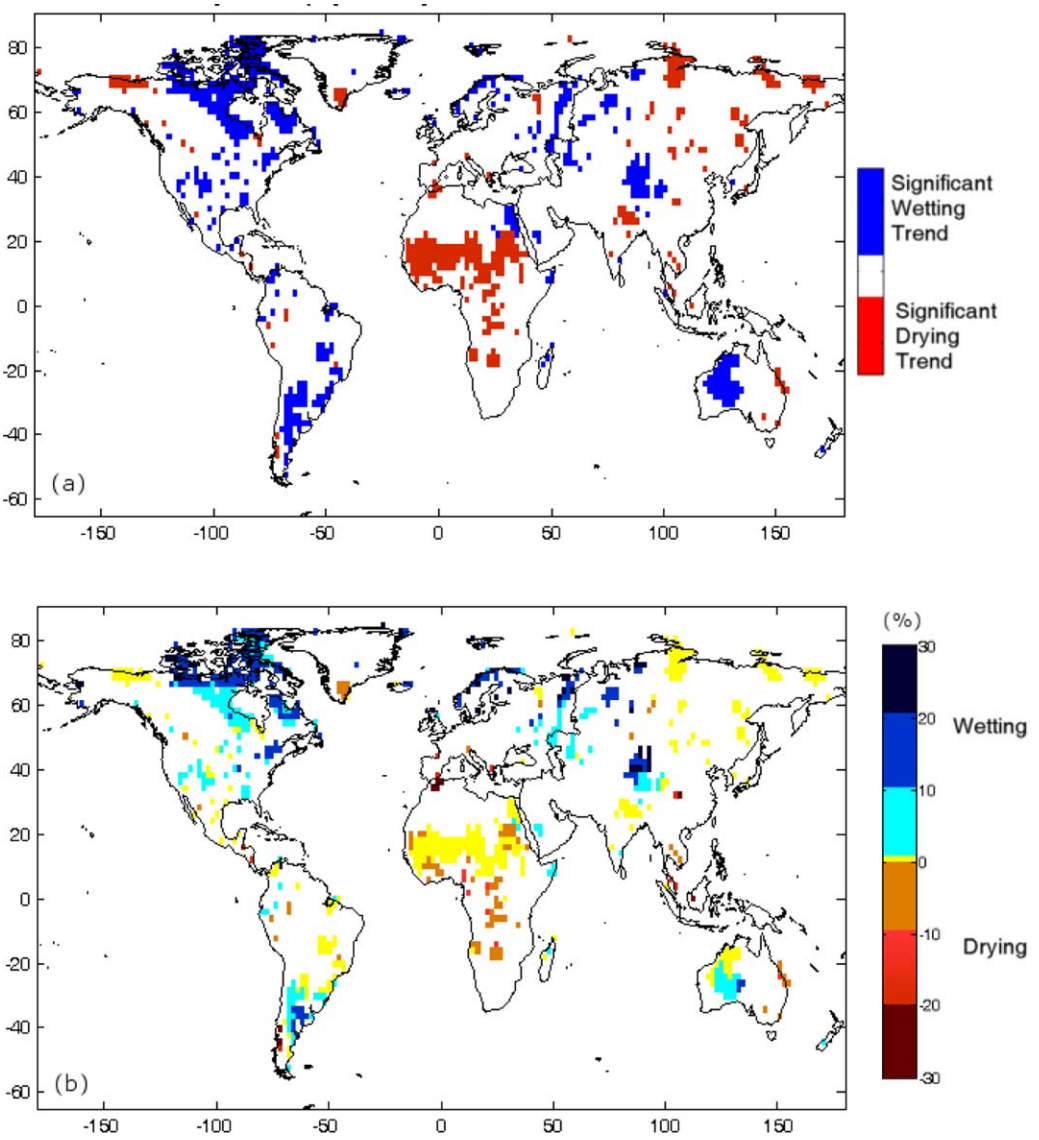

Figure 4. (a) Significant positive (bluish colors) or negative (reddish colors) trend in the CRU observations based on mean annual precipitation for the period 1950–2005. (b) Percent of CMIP5 simulations with wetting or drying trends that are in statistically significant agreement with the CRU data for this period.

other hand, the eastern part of Australia, north-eastern Asia, and most of Africa show drying trends, with the largest area of drying occurring in western, sub-Saharan Africa.

Having identified significant trends in the observations, the same analysis procedure was applied to 41 CMIP5 climate model simulations. Instead of plotting individual model results at pixel scale, the number of models that exhibit significant drying or wetting trend similar to the CRU data is presented in Figure4b which plots the percent of CMIP5 simulations that are in agreement with significant wetting or drying trends in the CRU data set. Overall, the models show weak agreement with the observed wetting and drying trends. At most, about 35% (14 out of 41) of the simulations are in agreement with the observed wetting trend over northern Canada, and most of the CMIP5 models do not display the significant drying trend in CRU precipitation observed over the western sub-Saharan Africa.

Most parts of the globe do not exhibit any statistically significant precipitation trend based on post-1950 CRU observations (Figure 5a). In contrast to those regions with observed significant trends (Figure 4b), the CMIP5 simulations are in better agreement with the observed no-trend regions (Figure 5b). Eastern Russia, northeastern China, central South America, and the northern United States are areas that almost all climate

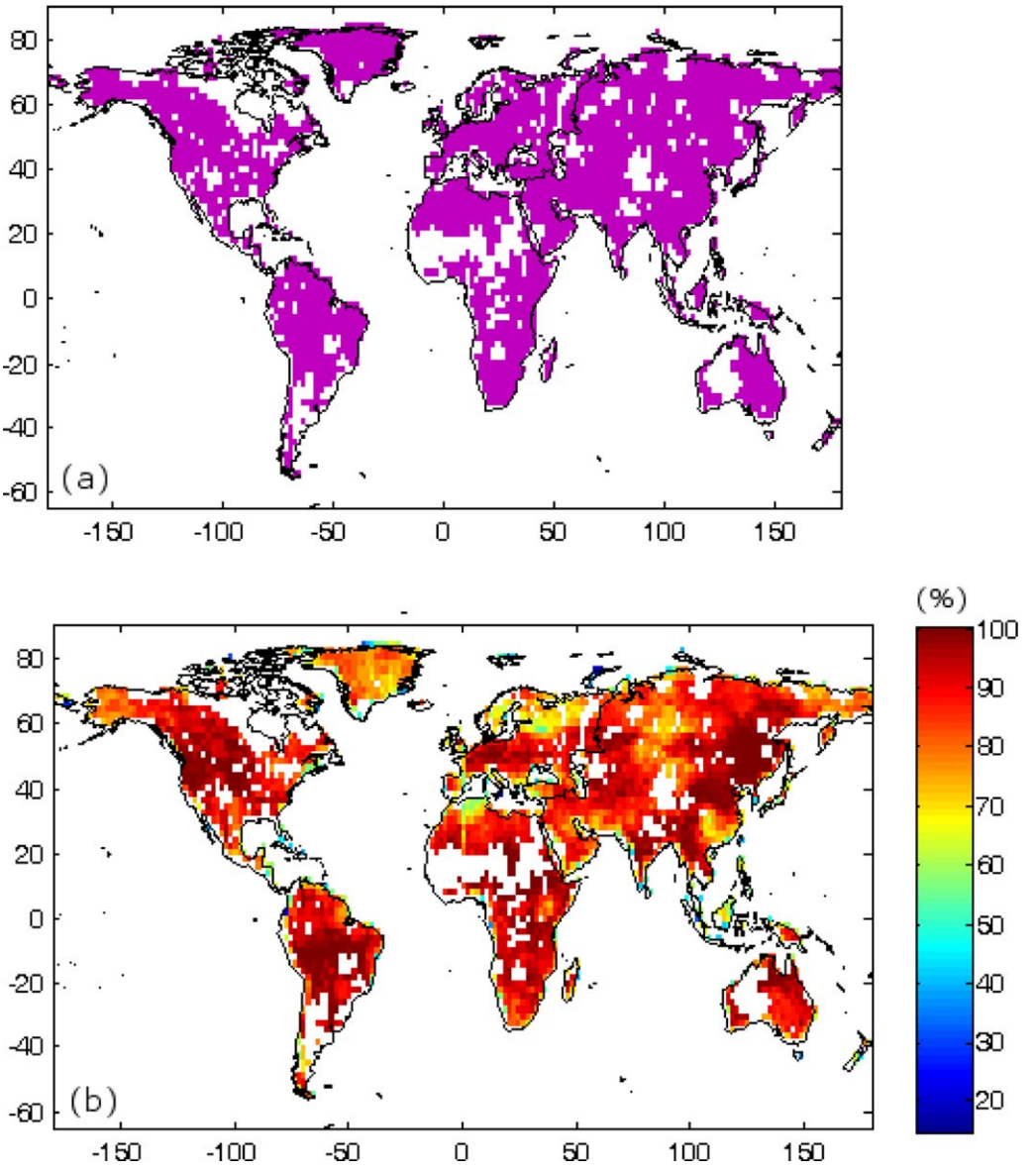

Figure 5. (a) Spatial distribution of areas without any significant trend in the CRU precipitation data over the period 1950–2005. (b) Percent of models in agreement with no significant trend in the observations for the period 1950–2005.

simulations display the same trend as that of the CRU precipitation data. In general, the models agree with the observations over more than 70% of the global land area. When considering observational data over the entire 1900–2005 observation period, the areas with significant trends change slightly (not shown, for brevity); however, the overall behavior of models relative to observations remains similar.

The trend in the mean annual precipitation provides information on slower changes in precipitation, but it does not provide insights about seasonal changes in the data. To address this issue, trends in the 3 month SPI were also analyzed, where the nonoverlapping 3 month SPI for the months of January to March, April to June, July to September, and October to December were considered for trend analysis. Figure 6a presents the spatial distribution of significant trends in the 3 month SPI for the CRU data. Overall, the spatial distribution of trend is similar to the annual trend of the CRU data set. Figure 6b displays the percentage of CMIP5 models that are in agreement with the significant trend in the CRU data set over each pixel, but greater agreement is found in higher latitudes. In most locations, the model-observational agreement is less than 10%; however, a large portion of the land area shows no significant trend in the CRU data (Figure 7a), and, in this respect, the CMIP5 precipitation simulations are in generally good agreement with the observations

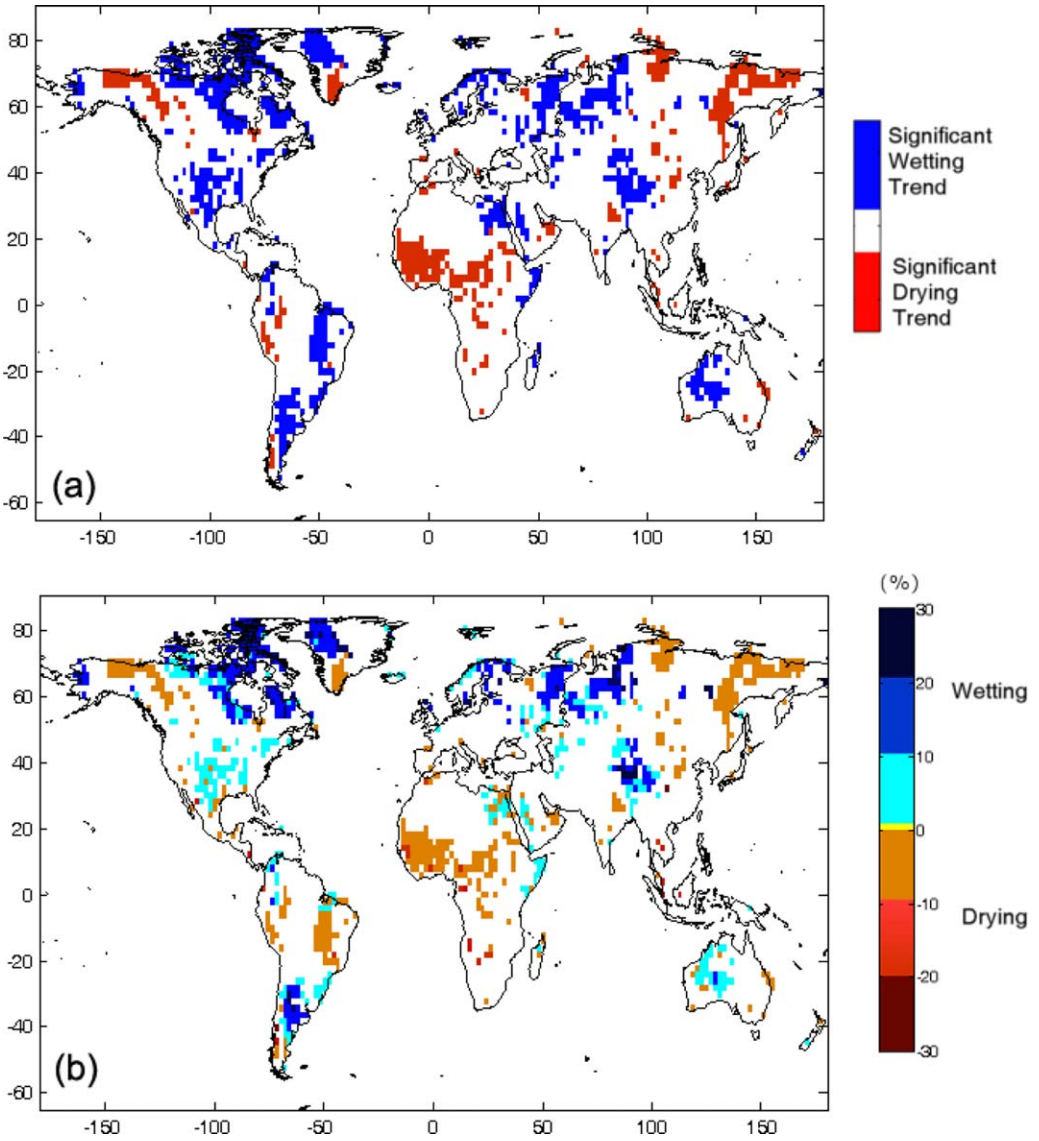

Figure 6. (a) Significant positive (blue) or negative (red) trend in the CRU precipitation observations for the period 1950–2005, based on the 3 months SPI. (b) Percent of model simulations with significant wetting or drying trend in agreement with the CRU data for the same period.

(Figures 7a and 7b). Similar results are also observed in nonoverlapping 6 month SPI data (see supporting information Figures S3 and S4).

The patterns of drying and wetting trends in the CMIP5 simulations also vary greatly among different models. In general, spatial differences among models are expected at pixel scale; however, on regional scale, the patterns of significant trends in simulation data sets are expected to display more similarity with the observations. Figure 8 shows the drying and wetting trends in the CRU data as well as in a subset of CMIP5 simulations. While some models tend to show wetting patterns over large areas of high latitudes (e.g., BCC-CSM1_1), others (e.g., CESM1-BGC_esm) show only a spatially limited wetting pattern over the same region. Moreover, none of the models presented in Figure 8 show the consistent drought observed in the northern part of Sub-Saharan Africa that is attributed to the Atlantic sea surface temperature gradients [*Servain et al.*, 2000]. On the contrary, the HadGEM2-ES_esm and FGOALS-S2 model simulations instead display a significant wetting trend over this region. The CRU data also show a significant wetting trend over Western Australia that is only partially present in the BCC-CSM1-1_esm and IPSL-CM5A-LR model simulations. In addition, Figures 8e and 8f also display the extensive differences exhibited by the FGOALS-g2 and FGOALS-

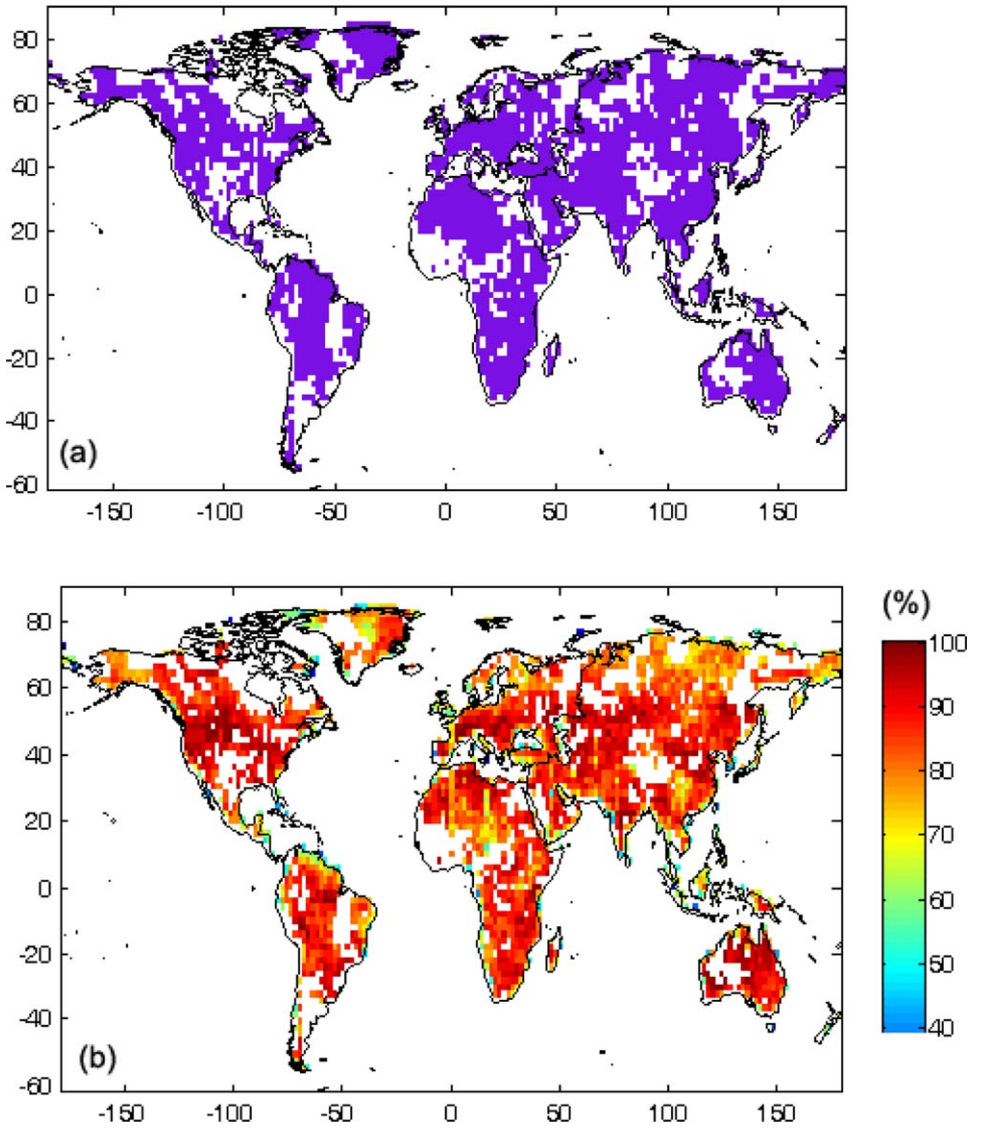

Figure 7. (a) Spatial distribution of areas without any significant trend in the CRU data based on 3 months SPI for period 1950–2005. (b) Percent of models in agreement with no significant trend in the observations for the same period.

s2 climate models, which include similar land and ocean components, but different atmospheric models. It should be noted, however, that some intermodel differences are not intrinsically "physical," but are also stochastic in character: Because individual CMIP5 simulations are started from somewhat different initial/boundary conditions of their ocean, land, and atmospheric model components, the spatiotemporal evolution of each climate simulation will also be somewhat different. Further details of CMIP5 intermodel precipitation differences are discussed in *Zhou et al*. [2013].

In addition to examining the regional changes of the trend, the latitudinal changes of the land area under drought are also investigated and presented here. Figure 9 assesses the latitudinal and decadal changes of the land area under moderate drought (6 month SPI ≤ -1)—see also supporting information Figure S5 for 3 month SPI ≤ -1. In most latitudes, the CMIP5 models encompass the temporal changes in the area under moderate drought. However, the variability of the area under drought is not well represented in the models, especially over both low and high latitudes. In general, the model areas under drought vary more smoothly with latitude than do the CRU observations. While the ground-based observations show nearly 60% of the land under moderate drought on the area of 50°S latitude during 1985–1995, the models (with less than 30% of the land area at this latitude under drought) could not adequately capture this extensive extreme.

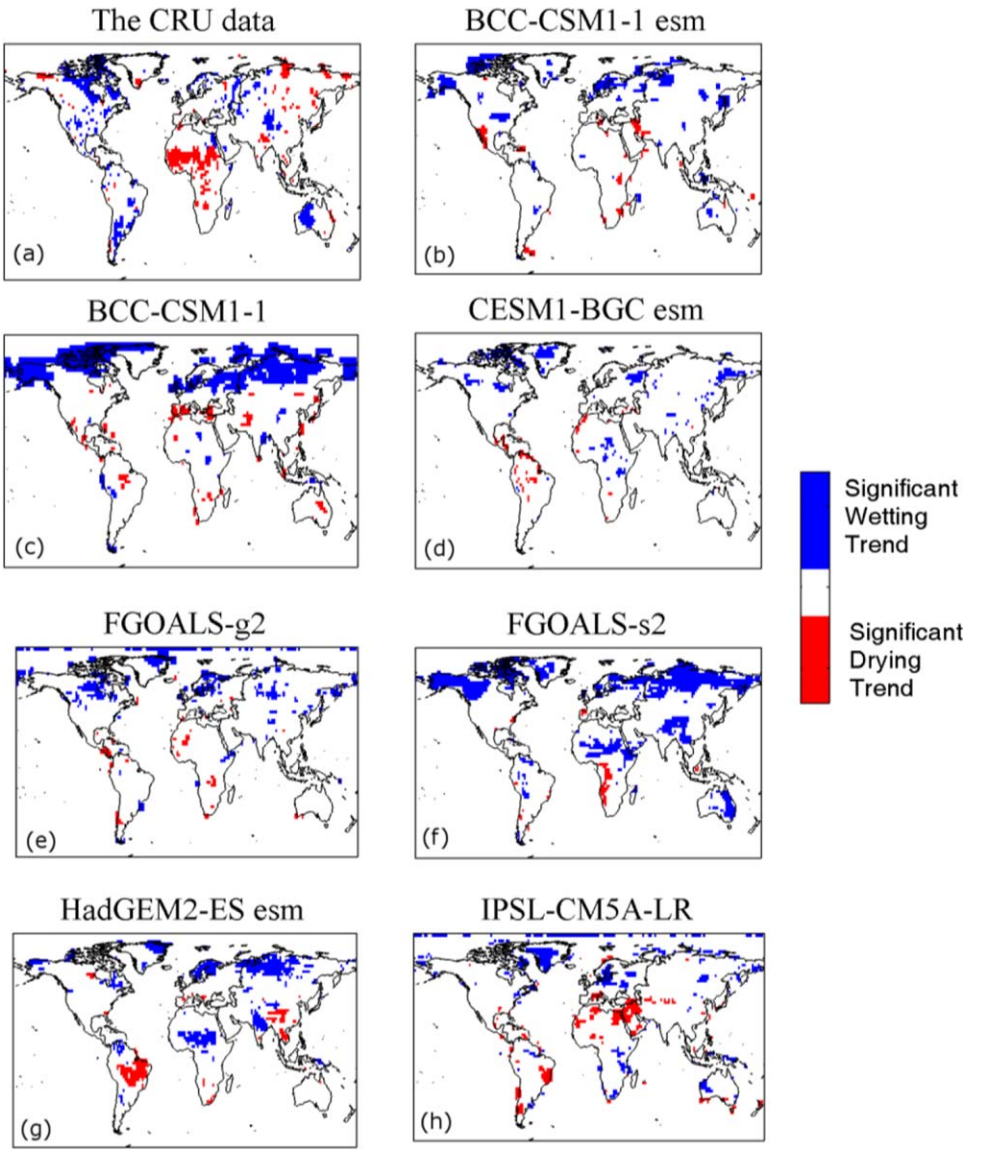

Figure 8. Significant positive (bluish colors) or negative (reddish colors) trend in the CRU observations based on mean annual precipitation for the period 1950–2005. (b–h) Subset of CMIP5 simulations with wetting or drying trends for this period.

The last decade of the study period (1995–2005) shows the best agreement between NH observations and model simulations; however, there are large discrepancies in the SH between observation and models, with the latter overestimating the area under drought by a factor of 2. Examining the decadal variability of the area under moderate drought also shows some interesting variations in the latitudinal patterns of changes. For example, the changes during the period of 1925–1965 (plots c, d, e, and f) are very similar, as is the period 1975–1995 (plots h and i). In general, there is no distinct latitudinal pattern of percent area under drought during the 10 decades considered in this study. The latitudinal and decadal changes of the land area under moderate drought in both 3 and 6 month SPI are consistent (compare Figure 9 with supporting information Figure S5).

Investigating the regional differences between individual simulations and observations is very important for selecting a subset of models suitable for studies of a particular region, where model performance can vary greatly. To find the relatively "best" overall CMIP5 model considered here, the mean absolute difference between a model's monthly precipitation and that of the CRU observations is calculated at each $2^\circ \times 2^\circ$ grid cell during 1950–2005, with the model displaying the least difference being selected as the relatively

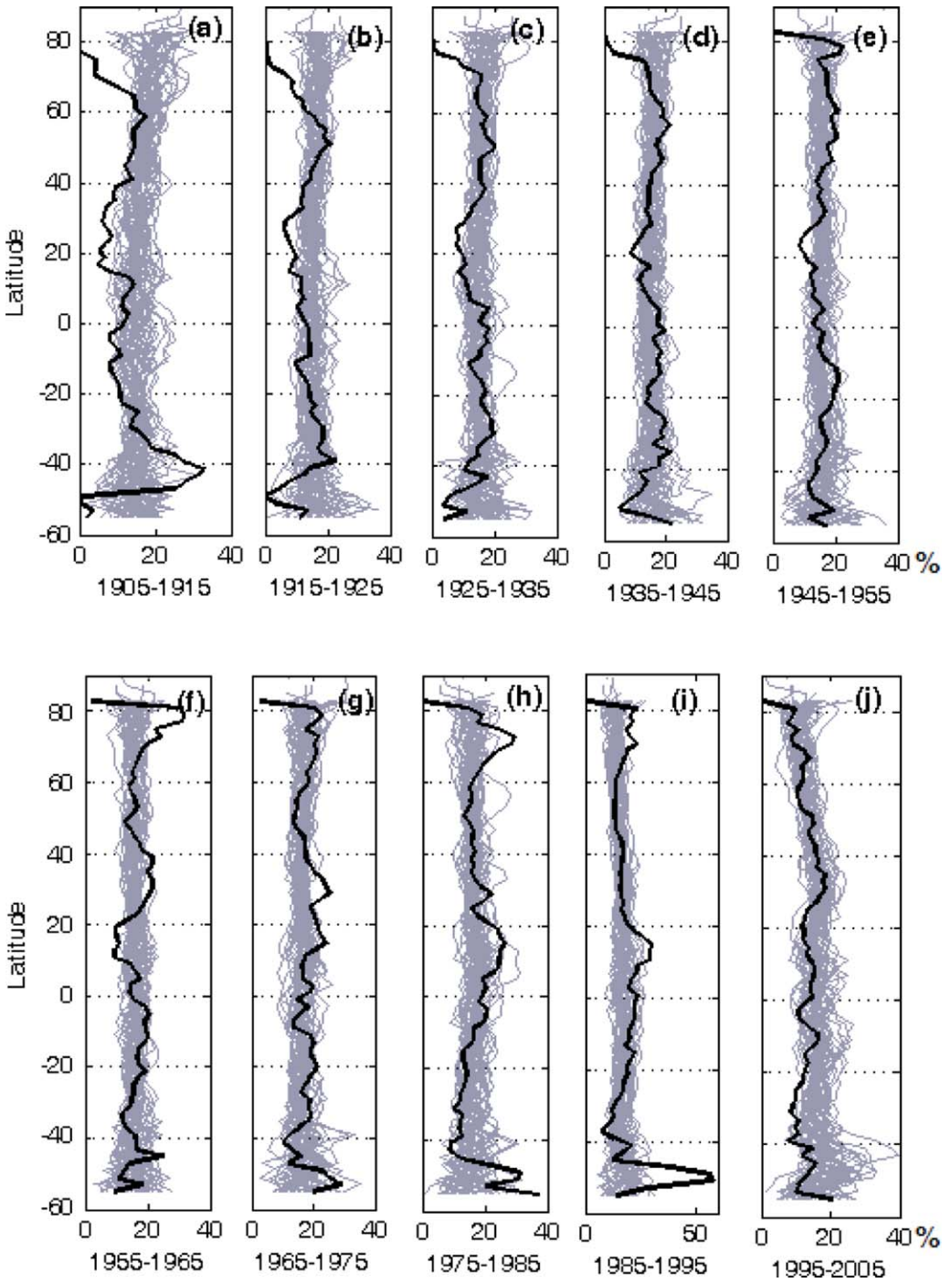

Figure 9. Latitudinal dependence of decadal changes of percentage (%) of land area experiencing moderate drought (6 month SPI ≤ -1). Black lines denote the values derived from the CRU precipitation observations, and gray shading the envelope of 41 CMIP5 simulations.

"best" model at that pixel. The results are presented in Figure 10, which indicates that there is no overall "best" model on a regional scale. For instance, models INMCM4-esm, MIROC5, and HadGEM2-CC show the best performance over parts of Greenland, northern Canada, and Australia, respectively. Overall, CNRM-CM5, FGOALS-g2, and MIROC5 showed the least mean absolute difference with CRU observations when aggregated over all grid cells, while models CCSM4 and MIROC-ESM-CHEM showed the largest mean absolute difference. Given that random pattern of the relatively "best" model in space (Figure 10), we argue that no one model could be selected as relatively "best" for any specific region. It should be noted that the differences between CMIP5 model simulations and observations are typically substantial (see, for example,

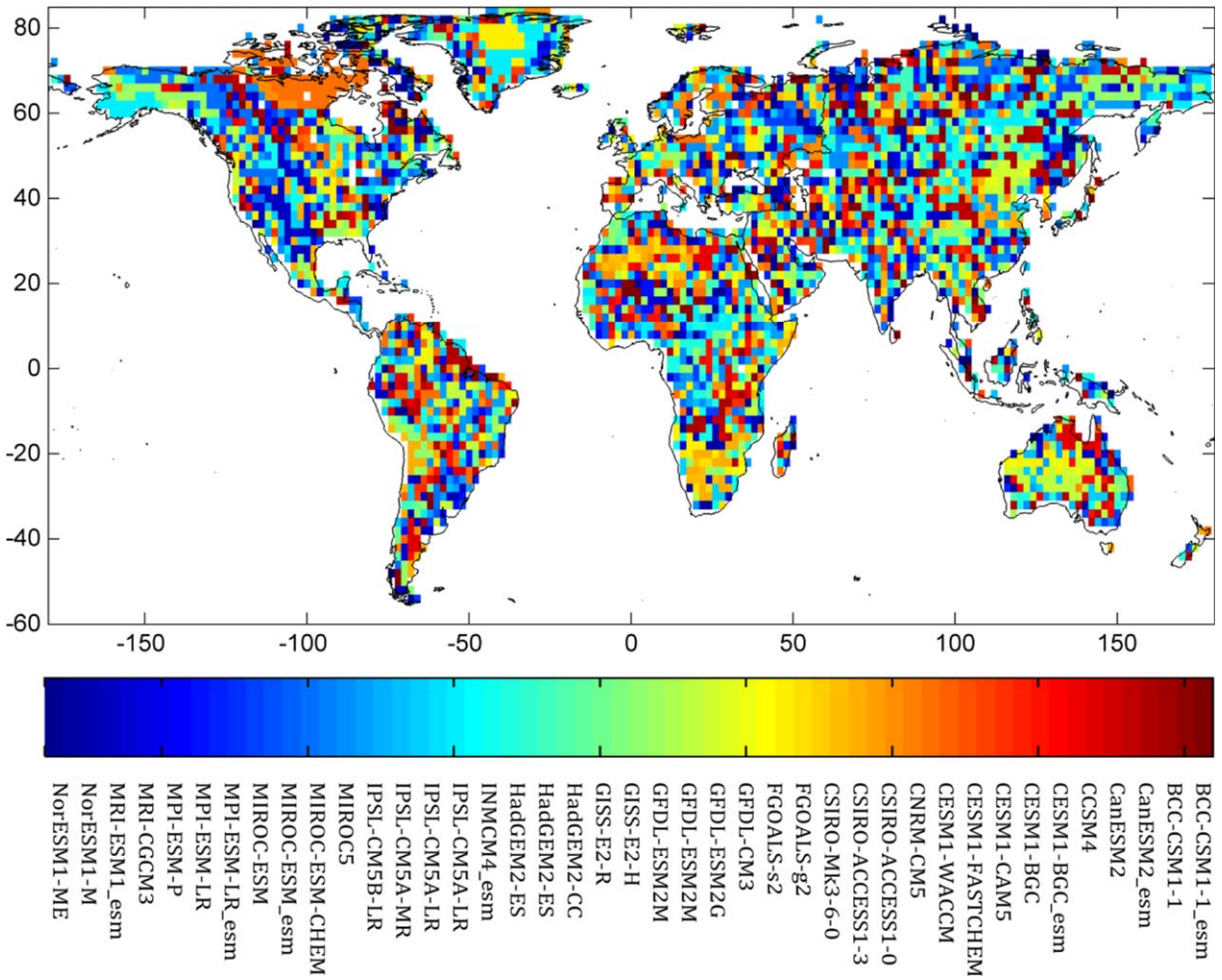

Figure 10. CMIP5 model with the least error (mean absolute difference) relative to CRU data at each $2^\circ \times 2^\circ$ grid cell. Lack of a consistent spatial pattern indicates that no single model can be considered as the "best" model for a certain region. The term "best" model is relative and only refers to the model that leads to the least error among the others at each pixel.

CMIP5 biases reported in *Liu et al*. [2014]). In this paper, the term "best" model is relative and only refers to the model that leads to the least error among the others.

As mentioned in section 3, the Kullback-Leibler (KL) divergence test is used to investigate changes in the distribution of precipitation in the climate models against the CRU observations. The results presented in Figures 4–8 showed that when considering the entire distribution of precipitation, limited areas exhibit significant drying or wetting trends in model simulations and observations. Similarly, when considering the entire distribution of precipitation, the KL test does not indicate statistically significant differences between model simulations and observations (not shown for brevity). However, the distributions of low precipitation are not reproduced very well in climate model simulations. Figure 11 displays the discrepancies between the distributions of the CMIP5 model simulations and that of the CRU observations for different thresholds of precipitation less than 10th (Figure 11a) and 30th (Figure 11b) percentiles. This figure shows percent of the models in which their low precipitation distributions exhibit statistically significant (0.05 significance level or 95% confidence) divergence compared to the corresponding distributions in the CRU precipitation. This indicates that the discrepancies between CMIP5 precipitation simulations and observations are more pronounced in the low thresholds. At a low threshold of precipitation less than tenth percentile, for example, most models do not agree with the observations. As the threshold increases, the discrepancies between the distributions of the model simulations and observations reduce (compare Figure 11a with Figure 11b). It should be noted that to reduce the effect of biases in model simulations relative to the observations, the percentiles are computed for each model and observations separately.

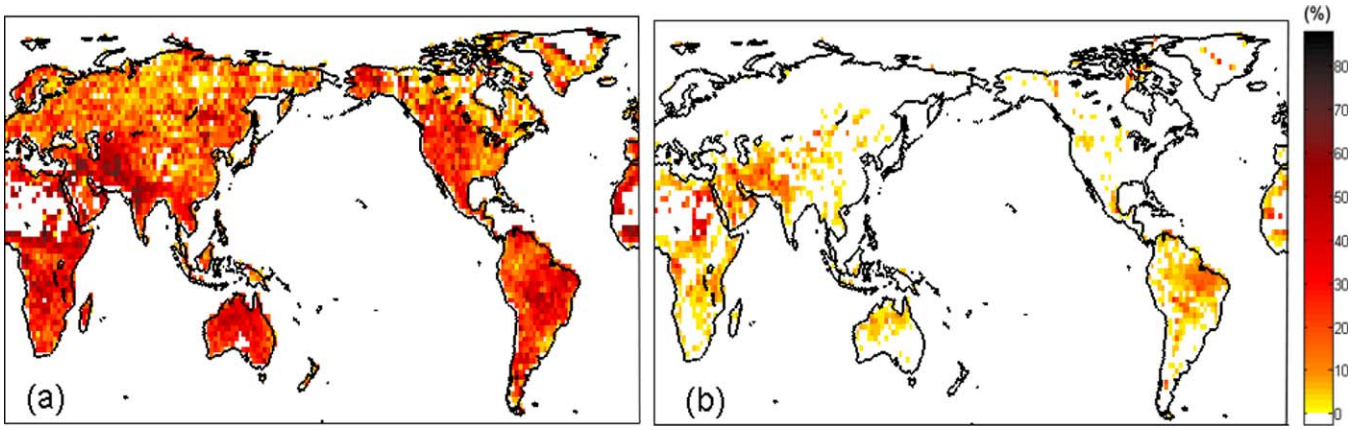

Figure 11. Percent of the CMIP5 model simulations that their distributions of precipitation less than (a) 10th and (b) 30th percentiles exhibit statistically significant (0.05 significance level) divergence compared to the distributions of CRU precipitation below the same thresholds (i.e., their distribution functions are significantly different from each other).

Previous studies indicate the drought assessment relies on the choice of drought indicator, and using different drought indices can lead to different results [*Burke and Brown*, 2008]. Given that the focus of this study is on meteorological drought, we have used SPI. In future studies, other drought indicators can be used to explore how CMIP5 model simulations represent droughts based on other drought definitions.

5. Conclusions and Remarks

The main motivation for efforts to simulate future climate is to provide a better understanding of anticipated changes to the Earth system. Assessing the uncertainties and understanding the deficiencies of climate models is fundamental to developing adaptation strategies for climate change [e.g., *Brekke and Barsugli*, 2012; *AghaKouchak et al*., 2012]. The objective of this study is to investigate how well CMIP5 climate model simulations replicate historical observations of the areas under drought, as well as significant wetting/drying trends, and their spatial patterns across the globe.

The results show that the CMIP5 multimodel simulation ensemble encompasses the Climatic Research Unit ground-based observations of areas under drought at all time steps. Overall, the CMIP5 global averages of area under drought during the last century correspond well with both CRU observations and previous studies. Furthermore, the results show that the time series of observations and CMIP5 simulations of areas under drought exhibit more variability in the Southern Hemisphere (SH) than in the Northern Hemisphere (NH). However, CMIP5 simulations substantially overestimate the observed variability, particularly in the SH.

The trend analysis of areas under drought reveals that the observational data exhibit a positive trend at a significance level of 0.05 over all land areas, as well as in the NH and SH. This result is reproduced by 78% of the CMIP5 models when considering total land areas in drought. Over the NH and SH, respectively, 78% and 66% of the CMIP5 climate models are consistent with the drought trends inferred from the CRU observations. Overall, the results show that most CMIP5 models agree with the observed global or hemispheric trends of areas under drought.

In addition to the fraction of land under drought, regional changes in the extreme precipitations were also investigated. The motivation for investigating both drought and wet conditions was to investigate consistencies and discrepancies in trends signals in model simulations and ground-based observations. The regional trends in the annual mean precipitation and also 3 month SPI (SPI3) data from CMIP5 models were compared to the trends in CRU data. Overall, CMIP5 simulations of regional trends are collectively in best agreement with high-latitude observations. However, the results show that the CMIP5 precipitation simulations do not generally agree well with observed regional drying and wetting trends. Over many regions, such as northeastern Asia and parts of central and western Africa, the CMIP5 simulations are not consistent with one another or with the observed trends. In fact, none of the CMIP5 models reproduced the significant drying pattern observed over central Africa and northeastern Asia. The model simulations not only fail to

accurately estimate the spatial patterns of drying and wetting trends, but they often exhibit trends with opposite signs than those observed. The results also show that many regions of the world do not exhibit any significant drying or wetting trend (both in annual and 3 month data). In this respect, most CMIP5 models are in agreement with the CRU precipitation observations.

The latitudinal and decadal changes of the percent of land area under drought were also investigated in this study. While there were changes in the models' collective ability to capture the moderate drought in different decades and over different latitudes, a distinct latitudinal pattern in the percentage of areas under drought was not evident over the past 10 decades. Grid-scale performance of all models was also investigated, and it was found that there is no specific region where one model simulation can be considered substantially superior to others. Furthermore, the results show that there are substantial discrepancies between the distribution functions of low-precipitation data (e.g., below tenth percentile) in CMIP5 model simulations and CRU observations.

A demonstrated ability to simulate large-scale and long-term observed trends and low precipitation distribution are fundamental for instilling confidence in model-based projections of future climate change. While it is recognized that the CMIP5 models cannot be expected to reproduce individual extreme events or other observational details on a monthly to annual time scale, they should be able to reproduce observed long-term precipitation trends, patterns and distributions. This study demonstrates that current-generation global coupled climate models have serious deficiencies in this regard, implying that much work in simulating the intensity and frequency of regional precipitation, as well as its local and remote moisture sources, still remains to be done.

Acknowledgments

This study is supported by the U.S. Army Research Office award W911NF-11-1-0422, the NOAA NCDC (Award NA09NES4400006, NCSU CICS Sub-Award 2009-1380-01), the National Aeronautics and Space Administration (NASA) award NNX15AC27G and the National Science Foundation award EAR-1316536. We acknowledge the World Climate Research Programme's Working Group on Coupled Modeling, which is responsible for CMIP, and we thank the climate-modeling groups for producing and making available their model output. For CMIP, the U.S. Department of Energy's Program for Climate Model Diagnosis and Intercomparison provides coordinating support and leads the development of software infrastructure in partnership with the Global Organization for Earth System Science Portals. The CMIP5 data used in this study are available to public from http://cmip-pcmdi.llnl.gov/cmip5/data_portal.html.

References

AghaKouchak, A. (2014), Entropy-copula in hydrology and climatology, *J. Hydrometeorol.*, *15*, 2176–2189, doi:10.1175/JHM-D-13-0207.1.

AghaKouchak, A., and N. Nakhjiri (2012), A near real-time satellite-based global drought climate data record, *Environ. Res. Lett.*, *7*(4), 044037.

AghaKouchak, A., D. Easterling, K. Hsu, S. Schubert, and S. Sorooshian (2012), *Extremes in a Changing Climate*, Springer, Dordrecht, Netherlands.

AghaKouchak, A., L. Cheng, O. Mazdiyasni, and A. Farahmand (2014), Global warming and changes in risk of concurrent climate extremes: Insights from the 2014 California drought, *Geophys. Res. Lett.*, *41*, 8847–8852, doi:10.1002/2014GL062308.

Alexander, L., and J. Arblaster (2009), Assessing trends in observed and modelled climate extremes over Australia in relation to future projections, *Int. J. Climatol.*, *29*(3), 417–435.

Ault, T. R., J. E. Cole, and S. St. George (2012), The amplitude of decadal to multidecadal variability in precipitation simulated by state-of-the-art climate models, *Geophys. Res. Lett.*, *39*, L21705, doi:10.1029/2012GL053424.

Balan Sarojini, B., P. A. Stott, E. Black, and D. Polson (2012), Fingerprints of changes in annual and seasonal precipitation from CMIP5 models over land and ocean, *Geophys. Res. Lett.*, *39*, L21706, doi:10.1029/2012GL053373.

Becker, A., P. Finger, A. Meyer-Christoffer, B. Rudolf, K. Schamm, U. Schneider, and M. Ziese (2013), A description of the global land-surface precipitation data products of the Global Precipitation Climatology Centre with sample applications including centennial (trend) analysis from 1901-present, *Earth Syst. Sci. Data*, *5*, 71–99.

Brekke, L., and J. Barsugli (2012), Uncertainties in projections of future changes in extremes, in *Extremes in a Changing Climate*, Springer, doi:10.1007/978-94-007-4479-011.

Burke, E. J., and S. J. Brown (2008), Evaluating uncertainties in the projection of future drough, *J. Hydrometeorol.*, *9*(2), 292–299.

Cai, W., A. Purich, T. Cowan, P. van Rensch, and E. Weller (2014), Did climate change-induced rainfall trends contribute to the Australian millennium drought?, *J. Clim.*, *27*(9), 3145–3168.

Dai, A. (2012), Increasing drought under global warming in observations and models, *Nat. Clim. Change*, *3*, 52–58, doi:10.1038/nclimate1633.

Damberg, L., and A. AghaKouchak (2014), Global trends and patterns of droughts from space, *Theor. Appl. Climatol.*, *117*(3), 441–448, doi:10.1007/s00704-013-1019-5.

Dragalin, V., V. Fedorov, S. Patterson, and B. Jones (2003), Kullback–Leibler divergence for evaluating bioequivalence, *Statistics in medicine*, *22*(6), 913–930.

Farahmand, A., and A. AghaKouchak (2015), A generalized framework for deriving nonparametric standardized drought indicators, *Adv. Water Resour.*, *76*, 140–145, doi:10.1016/j.advwatres.2014.11.012.

Fatichi, S. (2009), Mann-Kendall test, technical report, Dep. Ing. Civ. e Ambientale, Univ. degli Stud. di Firenze. http://www.mathworks.com/matlabcentral/fileexchange/25531-mann-kendall-test.

Feng, X., A. Porporato, and I. Rodriguz-Iturbe (2013), Changes in rainfall seasonality in the tropics, *Nat. Clim. Change*, *3*, 811–815 doi:10.1038/nclimate1907.

Fu, R., L. Yin, W. Li, P. A. Arias, R. E. Dickinson, L. Huang, and R. B. Myneni (2013), Increased dry-season length over southern Amazonia in recent decades and its implication for future climate projection, *Proc. Natl. Acad. Sci. U. S. A.*, *110*(45), 18,110–18,115.

Funk, C. (2011), We thought trouble was coming, *Nature*, *476*(7358), 7.

Golian, S., O. Mazdiyasni, and A. AghaKouchak (2014), Trends in meteorological and agricultural droughts in Iran, *Theor. Appl. Climatol.*, *119*, 679–688, doi:10.1007/s00704-014-1139-6.

Hao, Z., A. AghaKouchak, and T. J. Phillips (2013), Changes in concurrent monthly precipitation and temperature extremes, *Environ. Res. Lett.*, *8*(4), 034014.

Hao, Z., et al. (2014), Global integrated drought monitoring and prediction system, *Sci. Data*, *1*, 1–10.

Hayes, M., M. Svoboda, D. Wilhite, and O. Vanyarkho (1999), Monitoring the 1996 drought using the standardized precipitation index, *Bull. Am. Meteorol. Soc.*, *80*, 429–438.
Hayes, M., M. Svoboda, N. Wall, and M. Widhalm (2011), The Lincoln declaration on drought indices: Universal meteorological drought index recommended, *Bull. Am. Meteorol. Soc.*, *92*(4), 485–488.
Hoerling, M., et al. (2013), An interpretation of the origins of the 2012 Central Great Plains drought, report, Natl. Oceanic and Atmos. Admin., Drought Task Force. Available online at http://www.esrl.noaa.gov/psd/csi/factsheets/pdf/noaa-gp-drought-assessment-report.pdf.
Hoerling, M., J. Eischeid, A. Kumar, R. Leung, A. Mariotti, K. Mo, and R. Seager (2014), Causes and predictability of the 2012 Great Plains drought, *Bull. Am. Meteorol. Soc.*, *95*(2), 269–282.
Joetzjer, E., H. Douville, C. Delire, P. Ciais, B. Decharme, and S. Tyteca (2012), Evaluation of drought indices at interannual to climate change timescales: A case study over the Amazon and Mississippi river basins, *Hydrol. Earth Syst. Sci. Discuss.*, *9*(11), 13,231–13,249.
Kendall, M. (1976), *Rank Correlation Methods*, 4th ed., Charles Griffin., London, U. K.
Kenyon, J., and G. C. Hegerl (2010), Influence of modes of climate variability on global precipitation extremes, *J. Clim.*, *23*, 6248–6262.
Kharin, V. V., F. W. Zwiers, X. Zhang, and M. Wehner (2013), Changes in temperature and precipitation extremes in the CMIP5 ensemble, *Clim. Change*, *119*(2), 345–357.
Kullback, S., and R. Leibler (1951), On information and sufficiency, *Ann. Math. Stat.*, *22*, 79–86, doi:10.1214/aoms/1177729694.
Liu, Z., A. Mehran, T. J. Phillips, and A. AghaKouchak (2014), Seasonal and regional biases in CMIP5 precipitation simulations, *Clim. Res.*, *60*, 35–50, doi:10.3354/cr01221.
Mann, H. (1945), Nonparametric tests against trend, *Econometrica*, *13*, 245–259.
McKee, T., N. Doesken, and J. Kleist (1993), The relationship of drought frequency and duration to time scales, in *Proceedings of the 8th Conference of Applied Climatology*, pp. 179–184, Am. Meteorol. Soc., Anaheim, Calif.
Meehl, G., and S. Bony (2011), Introduction to CMIP5, *CLIVAR Exch.*, *16*(2), 4–5.
Mehran, A., A. AghaKouchak, and T. J. Phillips (2014), Evaluation of CMIP5 continental precipitation simulations relative to satellite-based gauge-adjusted observations, *J. Geophys. Res. Atmos.*, *119*, 1695–1707, doi:10.1002/2013JD021152.
Mitchell, T., and P. Jones (2005), An improved method of constructing a database of monthly climate observations and associated high-resolution grids, *Int. J. Climatol.*, *25*(6), 693–712.
New, M., M. Hulme, and P. Jones (1999), Representing twentieth-century space–time climate variability. Part I: Development of a 1961–90 mean monthly terrestrial climatology, *J. Clim.*, *12*, 829–856.
New, M., M. Hulme, and P. Jones (2000), Representing twentieth-century space-time climate variability. Part II: Development of 1901–96 monthly grids of terrestrial surface climate, *J. Clim.*, *13*(13), 2217–2238.
Orlowsky, B., and S. I. Seneviratne (2013), Elusive drought: Uncertainty in observed trends and short- and long-term CMIP5 projections, *Hydrol. Earth Syst. Sci.*, *17*, 1765–1781, doi:10.5194/hess-17-1765-2013.
Pascale, S., V. Lucarini, X. Feng, A. Porporato, and S. Hasson (2014), Analysis of rainfall seasonality from observations and climate models, *Clim. Dyn.*, doi:10.1007/s00382-014-2278-2.
Pérez-Cruz, F. (2008), Kullback-Leibler divergence estimation of continuous distributions, Information Theory, ISIT 2008, IEEE International Symposium on (pp. 1666–1670).
Peterson, T. C., P. A. Stott, and S. Herring (2012), Explaining extreme events of 2011 from a climate perspective, *Bull. Am. Meteorol. Soc.*, *93*, 1041–1067.
Polade, S. D., D. W. Pierce, D. R. Cayan, A. Gershunov, and M. D. Dettinger (2014), The key role of dry days in changing regional climate and precipitation regimes, *Sci. Rep.*, *4*, 4364, doi:10.1038/srep04364.
Prudhomme, C., et al. (2014), Hydrological droughts in the 21st century, hotspots and uncertainties from a global multimodel ensemble experiment, *Proc. Natl. Acad. Sci. U. S. A.*, *111*(9), 3262–3267.
Reifen, C., and R. Toumi (2009), Climate projections: Past performance no guarantee of future skill?, *Geophys. Res. Lett.*, *36*, L13704, doi:10.1029/2009GL038082.
Schubert, S. D., and Y. K. Lim (2013), Climate variability and weather extremes: Model-simulated and historical data, in *Extremes in a Changing Climate*, pp. 239–285, Springer, Dordrecht, Netherlands.
Servain, J., I. Wainer, H. L. Ayina, and H. Roquet (2000), The relationship between the simulated climatic variability modes of the tropical Atlantic, *Int. J. Climatol.*, *20*(563), 939–953.
Sheffield, J., and E. F. Wood (2008), Projected changes in drought occurrence under future global warming from multi-model, multi-scenario, IPCC AR4 simulations, *Clim. Dyn.*, *31*(1), 79–105, doi:10.1007/s00382-007-0340-z.
Sheffield, J., E. Wood, and M. Roderick (2012), Little change in global drought over the past 60 years, *Nature*, *491*(7424), 435–438.
Sheffield, J., et al. (2013), North American climate in CMIP5 experiments. Part I: Evaluation of historical simulations of continental and regional climatology, *J. Clim.*, *26*(23), 9209–9245.
Sillmann, J., V. V. Kharin, X. Zhang, F. W. Zwiers, and D. Bronaugh (2013), Climate extremes indices in the CMIP5 multimodel ensemble: Part 1. Model evaluation in the present climate, *J. Geophys. Res. Atmos.*, *118*, 1716–1733, doi:10.1002/jgrd.50203.
Svoboda, M., et al. (2002), The drought monitor, *Bull. Am. Meteorol. Soc.*, *83*(8), 1181–1190.
Tanarhte, M., P. Hadjinicolaou, and J. Lelieveld (2012), Intercomparison of temperature and precipitation data sets based on observations in the Mediterranean and the Middle East, *J. Geophys. Res.*, *117*, D12102, doi:10.1029/2011JD017293.
Taylor, K. E., R. J. Stouffer, and G. A. Meehl (2012), An overview of CMIP5 and the experiment design, *Bull. Am. Meteorol. Soc.*, *93*(4), 485–498.
Trenberth, K. E., A. Dai, G. van der Schrier, P. D. Jones, J. Barichivich, K. R. Briffa, and J. Sheffield (2014), Global warming and changes in drought, *Nat. Clim. Change*, *4*(1), 17–22.
Vittal, H., S. Karmakar, and S. Ghosh (2013), Diametric changes in trends and patterns of extreme rainfall over India from pre-1950 to post-1950, *Geophys. Res. Lett.*, *40*, 3253–3258, doi:10.1002/grl.50631.
Wehner, M. (2012), Methods of projecting future changes in extremes, in *Extremes in a Changing Climate*, Springer, Water Science and Technology Library, *65*, 2013, pp. 223–237, doi:10.1007/978-94-007-4479-0_8.
Wilhite, D. (2000), *Drought: A Global Assessment*, Routledge Pub., London, U. K.
Wuebbles, D., et al. (2013), CMIP5 climate model analyses: Climate extremes in the United States, *Bull. Am. Meteorol. Soc.*, *95*, 571–583, doi:10.1175/BAMS-D-12-00172.1.
Wuebbles, D. J., K. Kunkel, M. Wehner, and Z. Zobel (2014), Severe weather in the United States under a changing climate, *Eos Trans. AGU*, *95*(18), 149.

Yin, L., R. Fu, E. Shevliakova, and R. E. Dickinson (2013), How well can CMIP5 simulate precipitation and its controlling processes over tropical South America?, *Clim. Dyn.*, *41*(11–12), 3127–3143.

Yue, S., P. Pilon, and G. Cavadias (2002), Power of the Mann–Kendall and Spearman's rho tests for detecting monotonic trends in hydrological series, *J. Hydrol.*, *259*(1), 254–271.

Zhao, T., L. Chen, and Z. Ma (2014), Simulation of historical and projected climate change in arid and semiarid areas by CMIP5 models, *Chin. Sci. Bull.*, *59*(4), 412–429.

Zhou, T., F. Song, and X. Chen (2013), Historical evolution of global and regional surface air temperature simulated by FGOALS-s2 and FGOALS-g2: How reliable are the model results?, *Adv. Atmos. Sci.*, *30*(3), 638–657.